

Impacts of Image Contrast on High-NA EUV Mask Structure Optimization in Low-voltage Electron Beam Lithography

C.H. Liu*, Y.C. Li, H.Y. Tseng, C.C. Liu, Z.A. Ding

Department of Electrical Engineering, National Taipei University, Taipei, Taiwan

*E-mail: chliuzzh@mail.ntpu.edu.tw

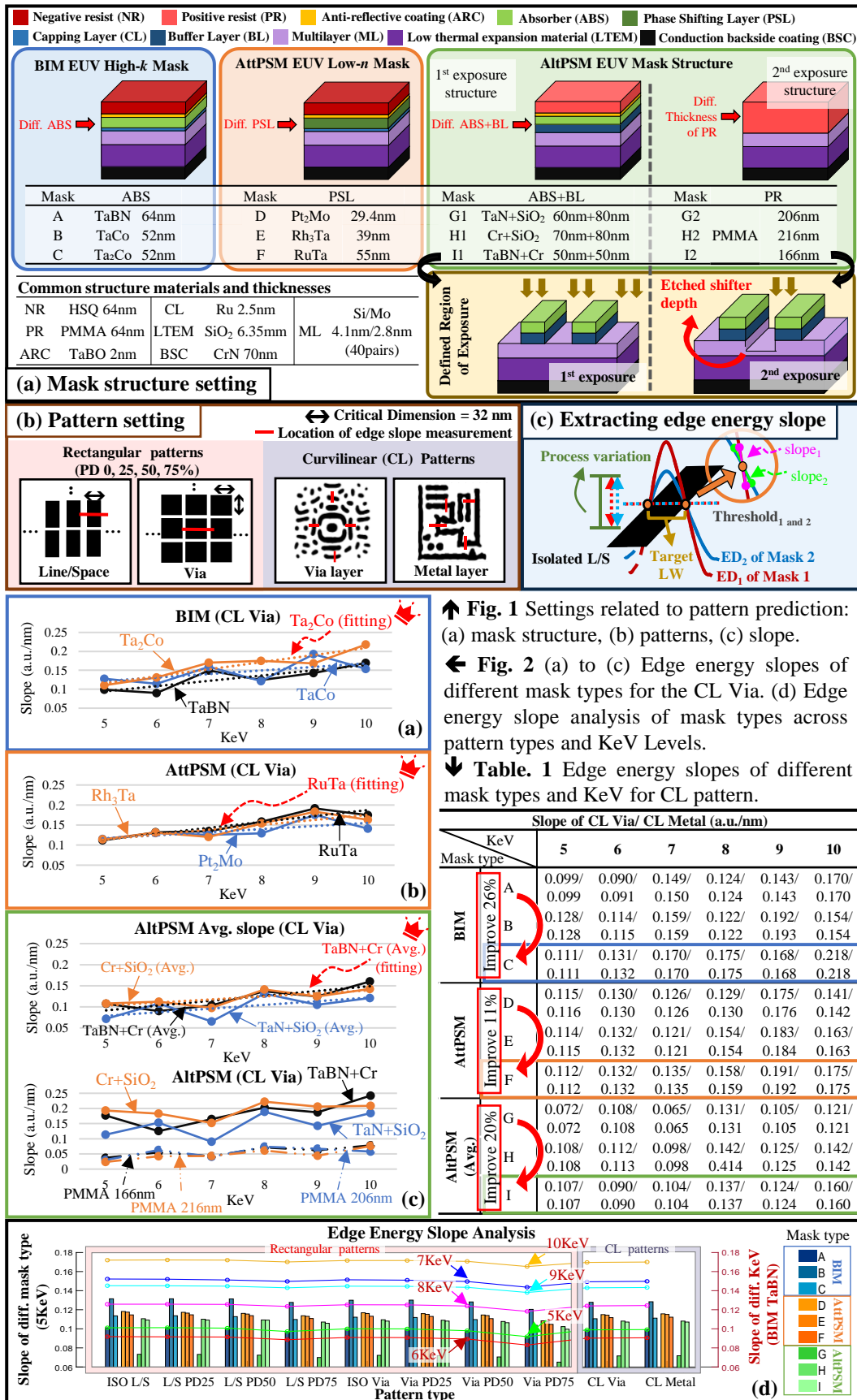
With the development of high numerical aperture (NA) extreme ultraviolet (EUV) lithography, research on novel absorber materials has focused on three directions: high extinction coefficient (k) induces a lower best focus range to mitigate phase impact; low refractive index (n) enhances the normalized image log slope; $n \approx 1$ reduces telecentric error and 2-bar critical dimension (CD) asymmetry.¹ To improve the imaging quality on the wafer side, it is essential to enhance mask imaging performance. In addition to mask resolution, image contrast, a critical metric for mask performance, enhances anti-process variation capability as contrast increases. This study investigates image contrast under various mask structures and pattern types, using the edge energy slope as its quantitative indicator to evaluate how image contrast affects mask-level performance. Each mask structure is designed with wafer-level consideration optimizations.²⁻⁴ Specifically, we (1) use the Monte Carlo method to simulate electron scattering in various mask structures, generating the absorbed energy distribution (AED) within the resist; (2) convolve the AED with different patterns to produce energy images; (3) apply different threshold values to define pattern contours by minimizing the normalized mean square error (NMSE). For rectangular patterns, including line/space and via patterns, the threshold matches the target CD. For curvilinear (CL) patterns, including via and metal layers, the threshold is determined through NMSE minimization; (4) extract, analyze and conclude the edge energy slope of the resulting patterns. Fig. 1 illustrates the settings used in pattern prediction. Fig 1(a) shows the mask structure settings, including the binary intensity mask (BIM), attenuated phase shift mask (AttPSM), and alternating phase shift mask (AltPSM). The red arrows indicate the specific layer structure variations among BIM (blue box), AttPSM (orange box), and AltPSM (green box), each of which uses appropriate $n-k$ value materials paired with respective optimized optical thickness. AltPSM involves two exposures, with the brown arrows indicating the regions defined during each exposure (brown box). Fig. 1 (b) presents the pattern settings, including rectangular and CL patterns. The black arrows mark the CD at 32 nm, while the red lines denote the location of the edge energy slope measurement. Fig. 1(c) shows edge energy slope extraction. Under process variation, a higher slope₁ reduces linewidth error. According to simulation results, Fig. 2 (a) to (c) illustrates the edge energy slopes of BIM, AttPSM, and AltPSM at different acceleration voltages (KeV), in which the black lines represent the baseline mask for each mask type, and the red arrows highlight the linear fitting results of the optimal structure for each mask type. The results of Fig. 2 indicate that (a) Ta₂Co overall outperforms the baseline mask (TaBN), (b) the baseline mask (RuTa) exhibits the best performance, (c) based on the average slope of the two-exposure structure, the linear fitting of the baseline mask (TaBN+Cr) is steeper than that of Cr+SiO₂. Fig. 2(d) shows the combined analysis of the edge energy slope: the bar chart illustrates the slopes of various masks for different pattern types at 5 KeV, in which blue, orange, and green are used to represent BIM, AttPSM, and AltPSM, respectively, and the line chart shows the slopes of the BIM baseline mask across different accelerating voltages for each pattern type. The analysis shows that (1) the slope decreases as pattern density increases, (2) the slope generally increases as KeV increases, and (3) changes in pattern types have no significant impact on the slope trends across different mask structures. Therefore, the optimal structure for each mask type applies to all pattern types. Table 1 summarizes the edge energy slopes of different masks for CL Via and CL Metal across various accelerating voltages. The highlighted boxes for mask C (Ta₂Co), mask F (RuTa), and mask I (TaBN+Cr) indicate the overall best-performing mask structure for BIM (blue), AttPSM (orange), and AltPSM (green), respectively. The slope improvements are 26%, 11%, and 20%, with mask C showing a 26% increase over mask A, mask F showing an 11% increase over mask D, and mask I showing a 20% increase over mask G. Currently, the study on the correlation between the edge energy slope and the trend of the AED itself is ongoing, aiming to directly predict the slope from the AED.

¹ V. Philipsen et al., in Photomask Technology 2018 (2018), Vol. 10810, pp. 53.

² D. Thakare et al., J. Micro/Nanopattern. Mater. Metrol. **22** (2023).

³ M. Wu et al., J. Micro/Nanopattern. Mater. Metrol. **20** (2021).

⁴ Y. Deng et al., in Emerging Lithographic Technologies VII (2003), Vol. 5037, pp. 302.



↑ Fig. 1 Settings related to pattern prediction: (a) mask structure, (b) patterns, (c) slope.

← Fig. 2 (a) to (c) Edge energy slopes of different mask types for the CL Via. (d) Edge energy slope analysis of mask types across pattern types and KeV Levels.

▼ Table. 1 Edge energy slopes of different mask types and KeV for CL pattern.

Slope of CL Via/ CL Metal (a.u./nm)						
KeV	5 6 7 8 9 10					
Mask type						
BIM	0.099/ 0.090/ 0.149/ 0.124/ 0.143/ 0.170/					
	0.099 0.091 0.150 0.124 0.143 0.170					
	0.128/ 0.114/ 0.159/ 0.122/ 0.192/ 0.154/					
AttPSM	0.128 0.115 0.159 0.122 0.193 0.154					
	0.111/ 0.131/ 0.170/ 0.175/ 0.168/ 0.218/					
	0.111 0.132 0.170 0.175 0.168 0.218					
AltPSM	0.115/ 0.130/ 0.126/ 0.129/ 0.175/ 0.141/					
	0.116 0.130 0.126 0.130 0.176 0.142					
	0.114/ 0.132/ 0.121/ 0.154/ 0.183/ 0.163/					
(Avg.)	0.115 0.132 0.121 0.154 0.184 0.163					
	0.112/ 0.132/ 0.135/ 0.158/ 0.191/ 0.175/					
	0.112 0.132 0.135 0.159 0.192 0.175					
(Avg.)	0.072/ 0.108/ 0.065/ 0.131/ 0.105/ 0.121/					
	0.072 0.108 0.065 0.131 0.105 0.121					
	0.108/ 0.112/ 0.098/ 0.142/ 0.125/ 0.142/					
(Avg.)	0.108 0.112 0.098 0.142 0.125 0.142					
	0.107/ 0.090/ 0.104/ 0.137/ 0.124/ 0.160/					
	0.107 0.090 0.104 0.137 0.124 0.160					

